A gyrokinetic ion zero electron inertia fluid electron model for turbulence simulations

Yang Chen and Scott Parker
Center for Integrated Plasma Studies, Department of Physics, University of Colorado at Boulder, Boulder, Colorado 80309

(Received 29 June 2000; accepted 31 October 2000)

This paper describes the formulation of a hybrid model with fully gyrokinetic ions and a zero-inertia fluid model for the electrons. The electron fluid equations are derived from moments of the drift kinetic equation, taking the small mass ratio limit, but with finite electron temperature. This model eliminates the inertial Alfvén wave and any physics relating to electron transit motion, making it useful for studying low frequency, high β ($\beta \gg m_e/m_i$) electromagnetic turbulence as well as kinetic magnetohydradynamics (MHD) physics including kinetic ballooning and toroidal Alfvén eigenmodes. Electromagnetic effects ($\delta \mathbf{B}_\perp$) are included through the parallel ion and electron current. A predictor-corrector scheme for the fluid part that is consistent with the gyrokinetic ion part has been developed. Here we derive the model equations, derive the linear kinetic-fluid theory in a three-dimensional shearless slab, and compare the simulation results with the linear theory. [DOI: 10.1063/1.1335584]

I. INTRODUCTION

The development of gyrokinetic simulations of turbulence and transport in tokamak plasmas with electromagnetic effects and nonadiabatic electron physics is a present-day research challenge. Over the past few years significant progress has been made. Simulations with kinetic electrons have been successfully applied to the study of Ion-Temperature-Gradient (ITG) driven instabilities,[1,2] internal kink modes[3,4] and collisionless reconnection.[5] The numerical difficulty associated with the calculation of the inductive component of the parallel electric field is solved by either using a generalized Ohm's law[1] or using the parallel canonical momentum formulation.[2,3] The electron free-streaming poses a constraint on the timestep, which is typically much smaller than that used in simulations with adiabatic electrons. Techniques for increasing the size of the time step, such as electron sub-cycling,[2] implicit moment methods[6] and, more recently, the development of the split-weight scheme,[7] have been successfully demonstrated for problems of lower dimensionality and simplified geometry.

Despite the progress toward direct simulations with kinetic electrons, simulations in realistic geometry and with plasma parameters remain a challenge. The time step achieved through the split-weight scheme,[7] as given by $k_\parallel v_{\mathrm{Te}} \triangle t \approx 1$, is still unnecessarily small compared with the time scale of drift waves or ITG instabilities. In addition, there are difficulties in extending the simulation to problems of higher dimensionality and large plasma β (or small magnetic skin depth).[2,8] In this paper we present an alternative electron model for studying electromagnetic effects. The primary goal is to obtain the electron parallel current for electromagnetic simulations, while eliminating electron transit motion, thereby avoiding any accuracy or stability constraints on $k_\parallel v_{\mathrm{Te}} \triangle t$, as well as electron free streaming noise. Hybrid simulations of this type with conventional particle-in-cell ions and conventional fluid equations have been used previously.[9–11] This hybrid approach has been suggested earlier[12–14] and similar drift-fluid electron equations have been used in electromagnetic gyrofluid simulations.[15] This approach provides a natural extension of previous electrostatic turbulence simulations to include the effects of electron $\mathbf{E}\times\mathbf{B}$ flow and the electron pressure gradient (i.e., ω_{*e} effects).

This model is useful because it is relatively simple and works well at high β. The purpose of this paper is to describe the model in general geometry as well as demonstrate its use in a simulation with three-dimensional (3D) shearless slab geometry where it can be easily compared with exact analytic linear theory. Fully toroidal results will be presented in a future paper. The dispersion relations for both the hybrid model and with fully kinetic ions and electrons in a shearless slab are derived and compared with simulation results. We will show that both the ITG instability and the shear Alfvén wave are included in the simpler hybrid model. Comparisons of the fully kinetic linear theory with the hybrid linear theory indicate that the hybrid model gives fairly good frequencies and growth rates. The paper is organized as follows. In Sec. II we discuss the model equations. In Sec. III the linear theory is discussed. Then in Sec. IV simulation results are presented and compared with the linear theory in Sec. III. Further details of the predictor-corrector algorithm for the fluid electron equations are given in the Appendix.

II. DRIFT-FLUID ELECTRON MODEL

In this section the drift-fluid electron model is discussed. The ions are treated as fully gyrokinetic using the fully nonlinear δf method. Details of how the ions are treated can be found in Refs. 16–20,1,2 and references therein.

We begin with the drift-kinetic equation for electrons

$$\frac{\partial fB}{\partial t}+\nabla\cdot\{fB[v_\parallel\tilde{\mathbf{b}}+\mathbf{v}_E+\mathbf{v}_D]\}+\frac{\partial}{\partial v_\parallel}\left\{fB\left[-\frac{e}{m_e}\tilde{\mathbf{b}}\cdot\mathbf{E}-\frac{\mu}{m_e}\tilde{\mathbf{b}}\cdot\nabla B+v_\parallel(\mathbf{b}\cdot\nabla\mathbf{b})\cdot\mathbf{v}_E\right]\right\}=0, \tag{1}$$

where $\tilde{\mathbf{b}}=\mathbf{b}+\delta\mathbf{B}_\perp/B$, $\mathbf{b}=\mathbf{B}/B$, $\mathbf{B}$ the equilibrium magnetic field, $\mathbf{v}_E=(1/B)\mathbf{b}\times\nabla\phi$, $\mathbf{v}_D=(v_\parallel^2+v_\perp^2)/(2/\Omega_e B^2)\mathbf{B}\times\nabla B$ which is valid for small β, $\beta\ll 1$. $\delta B_\parallel$ is also neglected. Integrating Eq. (1) over velocity we obtain the following continuity equation

$$\frac{\partial\delta n_e}{\partial t}+n_0(B\nabla_\parallel+\delta\mathbf{B}_\perp\cdot\nabla)\frac{u_{\parallel e}}{B}+\mathbf{v}_E\cdot\nabla(n_0+\delta n_e)+\frac{1}{m_e\Omega_e B^2}\mathbf{B}\times\nabla B\cdot\nabla(\delta P_\perp+\delta P_\parallel)+\frac{2n_0}{B^3}\mathbf{B}\times\nabla B\cdot\nabla\phi=0. \tag{2}$$

The momentum equation is obtained by multiplying Eq. (1) by $v_\parallel$ and integrating over velocity. Here we introduce the massless electron assumption: we formally allow $m_e\to 0$ but keep T_e and f finite. This is equivalent to assuming $v_A/v_{\mathrm{Te}}\to 0$ or $\beta_e m_i/m_e\gg 1$. Notice that this condition does not contradict the neglect of $\delta B_\parallel$ for typical tokamak plasmas. Then the lowest order terms are that from $\nabla\cdot v_\parallel\tilde{\mathbf{b}}Bf$ and $(\partial/\partial v_\parallel)fB[-(e/m_e)\tilde{\mathbf{b}}\cdot\mathbf{E}-(\mu/m_e)\tilde{\mathbf{b}}\cdot\nabla B]$. The mirror force term will be neglected, since we are mainly interested in passing electrons which carry most of the parallel current. The resulting equation is

$$en_0E_\parallel=-\tilde{\mathbf{b}}\cdot\nabla\delta P_\parallel-\frac{\delta\mathbf{B}_\perp}{B}\cdot\nabla(P_{\parallel 0e}-en_0\phi). \tag{3}$$

We will call this Ohm's law. The $(\delta\mathbf{B}_\perp/B)\cdot\nabla P_{\parallel 0e}$ term is important in reproducing the correct mode frequency when comparing to fully kinetic electrons. Equation (3) can be generalized to include collisional parallel resistivity and a Landau-fluid term to model collisionless dissipation,[21]

$$en_0E_\parallel=-\tilde{\mathbf{b}}\cdot\nabla\delta P_\parallel-\frac{\delta\mathbf{B}_\perp}{B}\cdot\nabla(P_{\parallel 0e}-en_0\phi)+\eta_e j_\parallel+\eta_{\mathrm{Lf}}(k_\parallel)n_0u_{\parallel\mathrm{e}}, \tag{4}$$

where $\eta_{\mathrm{Lf}}(k_\parallel)=(\sqrt{\pi}/2)(|k_\parallel|v_{\mathrm{te}}m_e/e)$. The appearance of $k_\parallel$ requires significant change to the numerical algorithm developed in this paper. Finite inertia effects can also be included by adding a linear term $n_o m_e\partial u_{\parallel\mathrm{e}}/\partial t$ to the righ-hand side of Eq. (3). In this paper only Eq. (3) is used.

We can continue taking higher moments of Eq. (1), however, for cases of small η_e, we can simply assume $\delta T_\perp\approx\delta T_\parallel\approx 0$, hence,

$$\delta P_\perp=\delta n_e T_{\perp 0}, \tag{5}$$

$$\delta P_\parallel=\delta n_e T_{\parallel 0}. \tag{6}$$

Snyder[15] has shown that when η_e is not small and electron thermal velocity is larger than the phase velocity for waves of interest, the electrons will rapidly thermalize along the perturbed magnetic field line. In such a case, it is appropriate to use a constant temperature along the perturbed magnetic field line

$$\tilde{\mathbf{b}}\cdot(T_{\mathrm{e}0}+\delta T_e)=0. \tag{7}$$

The electrostatic potential ϕ satisfies the quasi-neutrality condition,[17] which is in Fourier space,

$$\frac{1}{\lambda_D^2}(1-\Gamma_0(b))\phi=\frac{e}{\varepsilon_0}(\overline{\delta n_i}-\delta n_e), \tag{8}$$

where $b=(k_\perp\rho_i)^2$, $\lambda_D^2=(\varepsilon_0T_i/n_0e^2)$, $\overline{\delta n}_i$ is the gyro-averaged ion density. The vector potential is given by Ampere's law,

$$-\nabla_\perp^2A_\parallel=\mu_0(j_{\parallel i}-en_0u_{\parallel e}). \tag{9}$$

Then $\delta\mathbf{B}_\perp=\nabla A_\parallel\times\mathbf{b}$ and $\mathbf{E}=-\nabla\phi-(\partial A_\parallel/\partial t)\mathbf{b}$, and we use the following equation for $A_\parallel$:

$$\frac{\partial A_\parallel}{\partial t}=-\nabla_\parallel\phi-E_\parallel. \tag{10}$$

Equations (2), (3), (8)–(10), together with the gyrokinetic equation for ions, constitute the gyrokinetic-ion drift-fluid-electron hybrid model which is the topic of this paper.

III. LOCAL DISPERSION RELATION

In this section we derive the linear dispersion relation for the hybrid model as discussed in the previous section. This will give information regarding what type of waves and instabilities are contained within the model. The dispersion relation also provides a rigorous and analytically tractable result which we will use to validate the hybrid simulation model.

Consider a shearless slab where $\mathbf{B}=B_0\hat{\mathbf{z}}$. We will use $1/\omega_{\mathrm{ci}}$ for the unit of time, $\rho_i=m_iv_t/qB_0$ for the unit of length. The ion gyrokinetic equation, linearized around a Maxwellian background, $f_0=[n_0/(2\pi)^{3/2}v_t^3]\exp(-v^2/2v_t^2)$, is

$$\frac{\partial f}{\partial t_1}+v_\parallel\frac{\partial f_1}{\partial z}=-\left(v_\parallel\frac{\langle\delta B_x\rangle}{B_0}+\frac{\langle E_y\rangle}{B_0}\right)\frac{\partial f_0}{\partial x}-\frac{q}{m_i}\langle E_\parallel\rangle\frac{\partial f_0}{\partial v_\parallel}, \tag{11}$$

where $v_t=\sqrt{T_i/m_i}$ and $\langle\cdots\rangle$ denotes the gyro-average. The linear perturbed quantities have the form $\phi=\tilde{\phi}\exp(i\mathbf{k}\cdot\mathbf{x}-i\omega t)$, etc. The perturbed ion density and current are[1]

$$\frac{\delta n_i}{n_0}=L\Psi_1+M\Psi_2, \tag{12}$$

$$\frac{\delta j_i}{qn_0}=N\Psi_2, \tag{13}$$

with the following definitions

$$\Psi_1=\frac{\omega}{k_\parallel}A_\parallel, \tag{14}$$

$$\Psi_2=\phi-\frac{\omega}{k_\parallel}A_\parallel, \tag{15}$$

$$L=(\Omega-\Omega_T)\Gamma_0+\Omega_T\Gamma_*, \tag{16}$$

$$M=-\Gamma_0(1+\zeta Z)+(\tfrac{3}{2}\Omega_T\Gamma_0-\Omega_T\Gamma_*-\Omega\Gamma_0)\zeta Z -\Omega_T\Gamma_0\zeta^2(1+\zeta Z), \tag{17}$$

$$N=-\frac{\omega}{k_\parallel}[\Omega\Gamma_0(1+\zeta Z)+(-\tfrac{3}{2}\Omega_T\Gamma_0+\Gamma_0+\Omega_T\Gamma_*) \times(1+\zeta Z)+\Omega_T\Gamma_0(\tfrac{1}{2}+\zeta^2+\zeta^3 Z)], \tag{18}$$

where

$$\kappa_n=-\frac{1}{n_0}\frac{\partial n_0}{\partial x},\quad \kappa_T=-\frac{1}{T_i}\frac{\partial T_i}{\partial x},\quad \kappa_{\mathrm{Te}}=-\frac{1}{T_e}\frac{\partial T_e}{\partial x},$$

$\Omega=\kappa_n k_y/\omega$, $\Omega_T=\kappa_T k_y/\omega$, $\Gamma_0=\Gamma_0(b)=\Gamma_0(k_\perp^2 v_t^2/\Omega_i^2)$, $\Gamma_*=\Gamma_0-b(\Gamma_0-\Gamma_1)$. $\zeta=\omega/\sqrt{2k_\parallel v_t}$ and $Z(\zeta)$ is the plasma dispersion function.

The linearized continuity equation and Ohm's law using the normalized units are

$$\frac{\partial \delta n_e}{\partial t}+\nabla_\parallel u_{\parallel e}+\kappa_n\frac{\partial\phi}{\partial y}=0, \tag{19}$$

$$E_\parallel+\nabla_\parallel(\delta n_e+\delta T_e)-(\kappa_n+\kappa_{\mathrm{Te}})\delta B_x=0, \tag{20}$$

where $\beta=v_{\mathrm{ti}}^2/v_A^2$ and $v_A=B^2/\mu_0 n_0 m_i$ is the Alfvén velocity.

The electron temperature is given by Eq. (7)

$$\nabla_\parallel \delta T_e=\kappa_{\mathrm{Te}}\frac{\partial A_\parallel}{\partial y}. \tag{21}$$

Equations (19)–(21) are then combined with Eqs. (8) and (9) to give

$$k'^2_\perp\tilde{\phi}=\tilde{n}_i-\Psi_2-\frac{k_y}{\omega}\kappa_n\Psi_1, \tag{22}$$

$$k_\perp^2\tilde{A}_\parallel=\beta\left[j_{\parallel i}-\left(\frac{\omega}{k_\parallel}-\frac{k_y}{k_\parallel}\kappa_n\right)\Psi_2\right], \tag{23}$$

where $k'^2_\perp=1-\Gamma_o(b)$. Upon substituting the ion density and current, Eqs. (12) and (13), into Eqs. (22)–(23) the following dispersion relation is obtained:

$$k_\perp^2\frac{k_\parallel}{\omega}\left(M-\frac{1}{\tau}-k'^2_\perp\right)=-\beta\left(k'^2_\perp-L+\frac{k_y}{\omega}\kappa_n\right) \times\left(\frac{\omega}{\tau k_\parallel}-N-\frac{k_y}{k_\parallel}\kappa_n\right), \tag{24}$$

where $\tau=T_e/T_i$.

This is compared to the dispersion relation with fully-drift kinetic electrons[1] (assuming $T_e=T_i$ for simplicity)

$$-k_\perp^2\frac{k_\parallel}{\omega}(M-M_e-k'^2_\perp)=\beta(N_e-N)(k'^2_\perp-L+L_e), \tag{25}$$

where ($\Omega_{\mathrm{Te}}=\kappa_{\mathrm{Te}}k_y/\omega$ and $\zeta_e=\omega/\sqrt{2}k_\parallel v_{\mathrm{Te}}$)

$$L_e=\Omega,$$

$$M_e=1-(\Omega-\Omega_{\mathrm{Te}}/2-1)\zeta_e Z(\zeta_e)-\Omega_{\mathrm{Te}}\zeta_e^2(1+\zeta_e Z),$$

$$N_e=-\frac{\omega}{k_\parallel}\left[\Omega_{\mathrm{Te}}\left(\frac{1}{2}+\zeta_e^2(1+\zeta_e Z)\right) +(\Omega-\Omega_{\mathrm{Te}}/2-1)(1+\zeta_e Z)\right]. \tag{26}$$

With $k_\perp$ and $k_\parallel$ specified, Eq. (24) and Eq. (25) can be solved by searching the various complex domains for different modes. In particular, we find the generalized Newton's method[22] very useful for locating some of the modes. Write the dispersion relation as $D(\omega)=0$. For any complex ω we evaluate $\omega_0=\omega-D(\omega)/D'(\omega)$. ω (or ω_0) is close to a root if $|\omega-\omega_0|$ is sufficiently small.

Assuming $\zeta_e\ll 1$, $M_e\approx 1$ and $N_e\approx(\omega/k_\parallel)(1-\Omega)$, which is valid for the ITG and electron-drift-wave instabilities as well as for shear Alfvén waves at moderate β, ($\beta m_i/m_e>1$), Eq. (25) then reduces to Eq. (24). With $\beta=0$, Eq. (24) finally reduces to the following dispersion relation:

$$M-\frac{1}{\tau}-k'^2_\perp=0. \tag{27}$$

This is precisely the same dispersion relation one would get in the electrostatic case with adiabatic electron response $\delta n_e=\phi$. The right-hand side of Eq. (24) stands for the finite β effect. As will be seen numerically in Sec. IV, this finite β effect is always stabilizing for the slab ITG instability considered here. The ω_H mode, given by

$$\omega_H^2=\frac{k_\parallel^2}{k_\perp^2}v_{\mathrm{Te}}^2, \tag{28}$$

which appears in a fully kinetic treatment of electrons in zero-β limit,[23] does not appear in this hybrid model due to neglecting the electron inertia. The shear Alfvén wave is the highest frequency normal mode present. To see that the shear Alfvén wave *is* present, we take $L=M=N=0$. That is, neglecting the ion response except the ion polarization density in the gyrokinetic Poisson equation. We also assume a uniform plasma, $\kappa_n=\kappa_{\mathrm{Te}}=0$, and make the approximation $k'^2_\perp\approx k_\perp^2$ for small $k_\perp\rho_i$. Equation (24) then reduces to the usual shear Alfvén wave

$$\omega^2=k_\parallel^2 v_A^2(1+k_\perp^2\rho_s^2), \tag{29}$$

as expected.

In general, the constant temperature assumption along the field line should be used, Eq. (7). However, numerically inverting Eq. (7) is time-consuming, especially in toroidal geometry where complicated boundary conditions in the parallel direction are often employed. We note that, when linearized equations are used for the electrons, the electron temperature δT_e can be eliminated from Eq. (3) and Eq. (7). This approach is adopted in the simulations presented in this paper. The inversion of Eq. (7) is then avoided. Figure 1 shows the dispersion relation for the shear Alfvén wave with $k_x\rho_i=0.1$, $k_y\rho_i=0.3$, $k_\parallel\rho_i=7.14\times10^{-4}$. Other parameters are $\kappa_{\mathrm{Ti}}\rho_i=0.1$, $\kappa_{\mathrm{Te}}\rho_i=0$, $\kappa_n\rho_i=0.01$, $m_i/m_e=1837$. Results from both Eq. (25) and Eq. (24) are shown. For large β the two models agree, but at very low β the two differ due to

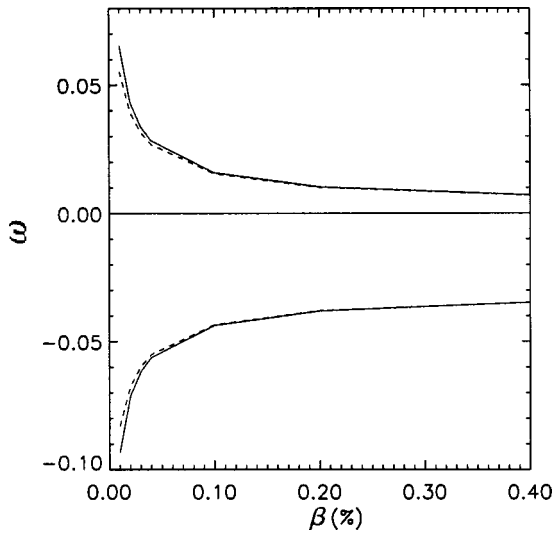

FIG. 1. Linear comparison of Alfvén frequency for the uniform plasma shear Alfvén wave from the hybrid and the fully-kinetic dispersion relations. Frequency of the mode versus β is shown.

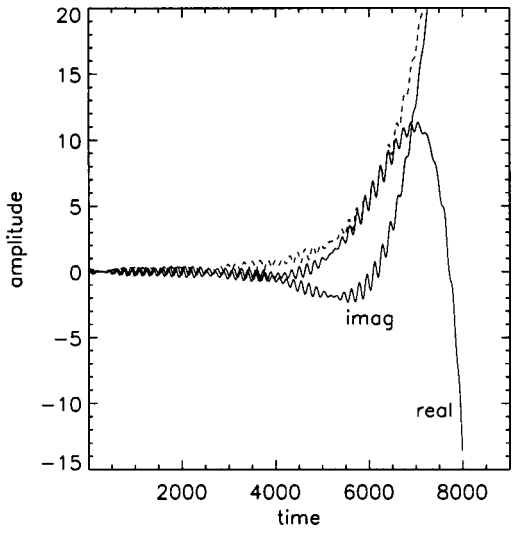

FIG. 3. Time history of one Fourier mode showing both the ITG mode and shear Alfvén wave fluctuations.

the existence of ω_H mode in the kinetic dispersion relation. Figure 2 shows the frequency and growth rate for the ITG mode. As can be seen, growth rates from the two models agree very well. It has been shown by Chen[24] that for $\kappa_{\mathrm{Te}}=0$ linearly the fluid electron model presented here agrees with electron equations derived using a rigorous perturbative treatment of the electrons based on the small parameter m_e/m_i.

IV. SIMULATION DETAILS AND RESULTS

A predictor-corrector scheme has been employed to integrate the model equations in time. Both the gyrokinetic Poisson equation (or quasi-neutrality condition) and Ampere's law are solved spectrally. A prominent feature of this scheme is that the Ampere's law is solved ''backwards,'' that is, $u_{\parallel e}$ is obtained from $A_\parallel$, which is evolved from Eq. (10). This scheme has also been tested in recent electromagnetic gyrofluid simulations by Snyder.[15] Snyder's simulations use a pseudo-spectral method. In the hybrid simulation presented here, it is impossible to take a fully spectral approach in the perpendicular plane as done with gyrofluid simulations because the particle trajectories are integrated in real space. Furthermore, simulating the ions with δf method introduces noise. As was shown in the previous section, the shear Alfvén waves can propagate even without the ion response (aside from the polarization density in the Poisson equation). The particle noise, once generated by the discrete ions, will persist and propagate in the simulation. The main purpose of this paper is to develop a 3D simulation in a simple shearless slab geometry where the comparison with exact analytical results is straightforward. An outline of the actual predictor-corrector scheme is given in the Appendix.

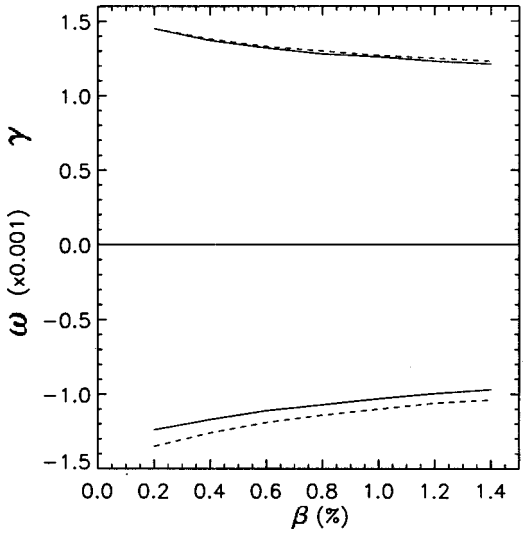

FIG. 2. Comparison of the ITG mode frequency and growth rate from hybrid and fully-kinetic linear dispersion relations as a function of β.

Ions are simulated using the δf method.[25,20,19] In a shearless slab, the evolution equation for the particle weights is

$$\dot{w}=-\frac{1}{g}\left[\left(\mathbf{v}_E+v_\parallel\frac{\langle\delta\mathbf{B}_\perp\rangle}{B}\right)\cdot\nabla f_M+\frac{q_i}{m_i}\langle E_\parallel\rangle\frac{\partial f_M}{\partial v_\parallel}\right], \qquad (30)$$

where f_M is the Maxwellian distribution, which is nonuniform in x direction. g is the numerically loaded particle distribution. Four-point averaging is used for gyro-averaging the perturbed field.[23] Particles are loaded uniformly in real space. In velocity space, both uniform loading (with a cutoff velocity well above the thermal velocity) as well as Maxwellian loading are used. The two loading schemes agree linearly, but uniform loading appears to be less noisy in the nonlinear phase of the simulation. The simulation is initialized with random particle weights, random electron density δn_e and vector potential $A_\parallel$ using ''quiet'' bit-reversed pseudo-random numbers.

Figure 3 shows the linear evolution of one Fourier mode with $k_x\rho_i=0.1$, $k_y\rho_i=0.3$, $k_\parallel\rho_i=7.139\times10^{-4}$. The gradi-

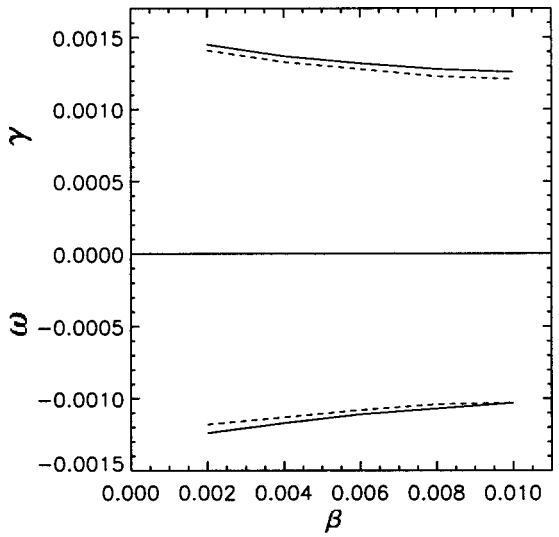

FIG. 4. Comparison of the hybrid simulation model with the growth rate and real frequency predicted by linear theory versus β.

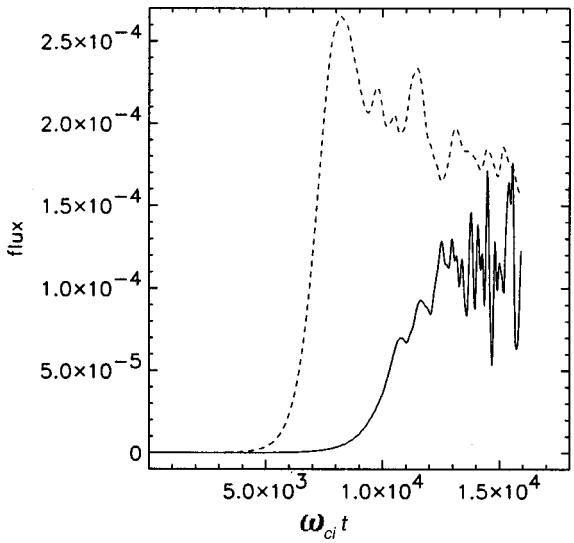

FIG. 5. Nonlinear simulations showing the heat flux versus time. The solid line is the electrostatic, adiabatic electron result and the dashed is the electromagnetic result with $\beta=0.01$.

ents are $\kappa_n\rho_i=0.01$, $\kappa_{\mathrm{Ti}}\rho_i=0.1$, $\kappa_{\mathrm{Te}}\rho_i=0$. The grid size is $N_x\times N_y\times N_z=64\times64\times16$ and the physical box size is $64\rho_i\times64\rho_i\times8796\rho_i$ with 262 144 simulation particles. The time step is $\Omega_i\triangle t=5$, which satisfied the Courant condition $k_\parallel v_A\triangle t<1$. Numerical tests indicate that violation of the Courant condition does indeed cause numerical instability. However, for moderate β (so that $v_A\ll v_{\mathrm{Te}}$) this condition can be easily satisfied, compared with the constraint $k_\parallel v_{\mathrm{Te}}\triangle t\leqslant1$ in kinetic simulations of electrons. As can be seen in Fig. 3, the Alfvén wave dominates in the early stage, then the unstable ITG mode grows and eventually dominates. Fourier analysis shows that the frequency of the fast oscillations is indeed in the range of the fast branch of the shear Alfvén frequency (see Fig. 1), which is $\omega_A=-3.3\times10^{-2}\Omega_i$ in this case. The complex frequency of the ITG mode is calculated from the dispersion relation to be $\omega_{\mathrm{ITG}}=(-1.03\times10^{-3},1.26\times10^{-3})\Omega_i$. The simulated result, estimated from Fig. 3, is $(-1.03\times10^{-3},1.21\times10^{-3})\Omega_i$, which is in very good agreement with the dispersion relation.

A more illustrative test of the simulation scheme is to show the finite β stabilization of the ITG instability. This has been difficult to observe in a two and three dimensional fully kinetic simulations.[8] The problem appears to be related to the resolution of the electron magnetic skin depth, which is inversely proportional to β.[2,26] To show significant stabilization of the ITG instability, the electron skin depth is typically a very small fraction of the ion gyroradius ($\sim\triangle x$ in gyrokinetic simulations of ITG modes), and this causes a resolution problem for kinetic simulations with electrons. For the hybrid simulation, the finite β stabilization is readily seen. Figure 4 shows the frequency and growth rate of the same ITG mode as in Fig. 3, but varying β. Results from both the dispersion relation and the hybrid simulation are shown. As can be seen, the agreement between the two is very good.

Finally, Fig. 5 shows the result of a simulation with nonlinear ion and linear electrons, i.e., keeping only linear terms in the fluid equations. When all the nonlinear terms are included in the electron equations, the simulation does not saturate well in a shearless slab geometry. The parameters are: $\kappa_n\rho_i=0.01$, $\kappa_{\mathrm{Ti}}\rho_i=0.04$, $\kappa_{\mathrm{Te}}\rho_i=0$. Modes with $k_\perp>1.0$ are filtered using a $e^{-k_\perp^4}$ filter applied to ion density and current. Also, to ensure full convergence, only Fourier components with $k_\parallel=0,\pm2\pi/L_z$ are retained in the simulation. The grid resolution is $N_x\times N_y\times N_z=64\times64\times64$ using the same physical box size as in Fig. 3. The time step is $\triangle t\Omega_i=4$, with 2 097 152 particles. The large number of particles and large N_z are necessary for a well-converged result. Figure 5 shows the evolution of energy flux for the adiabatic electron case (dashed) and the electromagnetic case with $\beta=0.01$. Consistent with the linear result, the nonlinear heat flux is lower in the electromagnetic case. Detailed analysis of nonlinear simulations, in particular simulations using a field-line-following flux tube simulation,[27,28] will be reported in a future paper.

V. SUMMARY

In this paper we presented a hybrid gyrokinetic-ion drift-fluid-electron model for the study of electromagnetic turbulence in tokamak plasmas. The motivation is to provide a very simple electron model that provides a parallel electron current and Alfvénic physics. This model is useful at high β and the electron transit motion does not need to be resolved numerically. This model could also be further extended to be used in combination with a drift-kinetic electron model. For example, one could close the electron fluid equations with δf_e from particles.[29–31] Another possibility would be to use this model for passing electrons and use a bounced-averaged model[32,33] or split-weight scheme[7] for trapped electrons. The model presented here *does* circumvent the problems associated with the fast free-streaming motion of electrons in a kinetic electron simulation, but it is a much simpler reduced physical description. This model may be useful for studying ITG instabilities where finite β effect is important and where the details of electron dynamics are not crucial. It was shown

here that for large η_i the hybrid model agrees fairly well with linear kinetic theory. An explicit predictor-corrector scheme has been developed and demonstrated by benchmarking the simulation results against linear theory for a shearless slab. We believe that the numerical scheme can also be applied to a flux tube geometry and such a code is under development. Results of toroidal simulations will be reported in future papers.

ACKNOWLEDGMENTS

We thank Dr. Liu Chen and Dr. Phillip Snyder for their useful suggestions. This work is supported by the U.S. Department of Energy, Office of Fusion Energy Sciences.

APPENDIX: OUTLINE OF THE PREDICTOR-CORRECTOR SCHEME

In this appendix we give a brief outline of the numerical scheme ($\mathbf{z}$ denotes ion coordinates) and the sequence in which quantities are calculated. In the following superscripts (n or $n+1$) denote the time step, tilde quantities denote the predicted values.

1. Predictor step

(1) push ions $\tilde{\mathbf{z}}^{n+1}=\mathbf{z}^{n-1}+2\triangle t\cdot\dot{\mathbf{z}}^{n}$

(2) integrate fluid equations

$$\delta\tilde{n}_e{}^{n+1}=\delta n_e^{n-1}+2\triangle t\cdot\left(\frac{\partial\delta n_e}{\partial t}\right)^n$$

$$\tilde{A}_\parallel{}^{n+1}=A_\parallel^{n-1}+2\triangle t\cdot\left(\frac{\partial A_\parallel}{\partial t}\right)^n$$

(3) calculate $(\widetilde{\delta n_i})^{n+1}$, $(\widetilde{\delta j_{\parallel i}})^{n+1}$ from particles

(4) solve Poisson equation $(\widetilde{\delta n_i})^{n+1},(\widetilde{\delta n_e})^{n+1}\rightarrow\tilde{\phi}^{n+1}$

(5) solve Ampere's law $\tilde{A}_\parallel{}^{n+1}\rightarrow(\widetilde{u_{\parallel e}})^{n+1}$ from Ampere's law

(6) $(\widetilde{\delta n_e})^{n+1},\tilde{A}_\parallel{}^{n+1}\rightarrow\tilde{E}_\parallel{}^{n+1}$ from Ohm's law

2. Corrector step

(1') push ions $\mathbf{z}^{n+1}=\mathbf{z}^n+0.5\triangle t\cdot(\dot{\mathbf{z}}^n+\tilde{\dot{\mathbf{z}}}^{n+1})$

(2') integrate fluid equations

$$(\delta n_e)^{n+1}=(\delta n_e)^n+0.5\triangle t\cdot\left(\left(\frac{\partial\delta n_e}{\partial t}\right)^n+\left(\widetilde{\frac{\partial\delta n_e}{\partial t}}\right)^{n+1}\right)$$

$$(A_\parallel)^{n+1}=(A_\parallel)^n+0.5\triangle t\cdot\left(\left(\frac{\partial A_\parallel}{\partial t}\right)^n+\left(\widetilde{\frac{\partial A_\parallel}{\partial t}}\right)^{n+1}\right)$$

(3') calculate δn_i^{n+1}, $j_{\parallel i}^{n+1}$ from particles

(4') solve Poisson's equation $\delta n_i^{n+1},\delta n_e^{n+1}\rightarrow\phi^{n+1}$

(5') solve Ampere's law $A_\parallel^{n+1}\rightarrow(u_{\parallel e})^{n+1}$ from Ampere's law

(6') $(\delta n_e)^{n+1},A_\parallel^{n+1}\rightarrow E_\parallel^{n+1}$ from Ohm's law

[1] J. Reynders, Ph.D. thesis, Princeton University, 1992.
[2] J. Cummings, Ph.D. thesis, Plasma Physics Lab, Princeton University, 1994.
[3] H. Naitou, K. Tsuda, W. Lee, and R. Sydora, Phys. Plasmas **2**, 4257 (1995).
[4] H. Naitou, K. Hironori, and S. Tokuda, J. Plasma Fusion Res. **73**, 174 (1997).
[5] R. Sydora and A. Rogister, in *Proceedings Joint Varenna–Lausanne International Workshop, Varenna* (Editrice Composotori for Societa Italiana di Fisica, Bologna, 1996).
[6] B. Cohen and A. Dimits, Phys. Rev. E **56**, 2151 (1997).
[7] I. Manuilskiy and W. Lee, Phys. Plasmas **7**, 1381 (2000).
[8] We have not been able to observe finite beta stabilization effect on ITG modes, using our 3D kinetic code with parallel canonical momentum formulation.
[9] J. Byers *et al.*, J. Comput. Phys. **27**, 363 (1978).
[10] D. E. Hewett, J. Comput. Phys. **38**, 378 (1980).
[11] D. Harned, J. Comput. Phys. **47**, 452 (1982).
[12] S. Parker, L. Chen, and W. Lee, Proceedings for the 15th International Conference on the Numerical Simulation of Plasmas (1994).
[13] S. Parker *et al.*, in *Joint Varenna–Lausanne International Workshop on Theory of Fusion Plasmas, August 22–26, 1994* (Editrice Composotori for Italiana di Fisica, Bologna, 1994).
[14] S. Parker, Y. Chen, and C. Kim, Comput. Phys. Commun. **127**, 59 (2000).
[15] P. Snyder, Ph.D. thesis, Princeton University, 1999.
[16] E. Frieman and L. Chen, Phys. Fluids **25**, 502 (1982).
[17] W. Lee, Phys. Fluids **26**, 556 (1983).
[18] T. Hahm, W. Lee, and A. Brizard, Phys. Fluids **31**, 2670 (1988).
[19] S. Parker and W. Lee, Phys. Fluids B **5**, 77 (1993).
[20] A. Dimits and W. Lee, J. Comput. Phys. **107**, 309 (1993).
[21] G. Hammett and F. Perkins, Phys. Rev. Lett. **64**, 3019 (1990).
[22] W. H. Press, S. A. Teukolsky, W. T. Vetterling, and B. P. Flannery, *Numerical Recipes in C* (Cambridge University Press, Cambridge, 1992), p. 347.
[23] W. Lee, J. Comput. Phys. **72**, 243 (1987).
[24] L. Chen, private communication (1999).
[25] M. Kotschenreuther, *Proceedings of the 14th International Conference on the Numerical Simulation of Plasmas* (Office of Naval Research, Arlington, VA, 1991), Paper PT20.
[26] B. Cohen, private communication (2000).
[27] M. A. Beer, S. C. Cowley, and G. W. Hammett, Phys. Plasmas **2**, 2687 (1995).
[28] C. C. Kim and S. E. Parker, J. Comput. Phys. **161**, 589 (2000).
[29] D. Barnes and R. Nebel, Bull. Am. Phys. Soc. **37**, 1557 (1992).
[30] J. Wang and J. Callen, Phys. Fluids B **4**, 1139 (1992).
[31] J. Callen, Bull. Am. Phys. Soc. **44**, 598 (1999).
[32] F. Gang and P. Diamond, Phys. Fluids B **2**, 2976 (1990).
[33] M. A. Beer and G. W. Hammett, Phys. Plasmas **3**, 4018 (1996).